Cosmic ray electron spectrum due to the dispersion of injection spectrum*

Tian-Lu Chen(陈天禄)[1,2,3] Wei Liu(刘伟)[4;1)] Qi Gao(高启)[2,3] Mao-Yuan Liu(刘茂元)[2,3]
Hai-Jin Li(厉海金)[2,3] Danzengluobu(单增罗布)[2,3] Ying Shi(石瑛)[1;2)]

[1] School of Physics and Technology, Wuhan University, Wuhan 430072,China
[2] Physics Department of the Science School, Tibet University, Lhasa 850000, China
[3] Key Laboratory of Cosmic Rays (Tibet University), Ministry of Education, Lhasa 850000, China
[4] Key Laboratory of Particle Astrophysics, Institute of High Energy Physics, Chinese Academy of Sciences, Beijing 100049, China

Abstract: The cosmic-ray total electron spectrum (electrons plus positrons) has been measured precisely up to TeV energies, with more interesting features found. Exhaustive analyses of the electron spectrum strongly support a spectral hardening above 100 GeV, rather than a featureless single power-law, which is confirmed by the most recent observations. Meanwhile, the measurements of the DAMPE satellite have verified the presence of a knee-like structure around 1 TeV in the electron spectrum, resembling the cosmic-ray knee. In this paper, we establish a physical model in which the observed electron spectrum is composed of a superposition of CR sources with various spectral indices and high-energy cutoffs. The dispersion of the power index is assumed to be Gaussian, while the cutoff energy E_c follows a power-law distribution. These simple ideas can account naturally for both the hundred-GeV excess and the TeV spectral break.

Keywords: electron, spectrum, cosmic rays, source, DAMPE

PACS: 95.85.Pw, 98.70.Sa **DOI:** 10.1088/1674-1137/42/7/075001

1 Introduction

Over the past dozen years or also, cosmic-ray electrons (CREs) (electrons plus positrons) have drawn extensive attention in the community. Subject to severe energy losses from synchrotron radiation and inverse Compton scattering during their diffusive transport, energetic CREs are widely believed to be from a relatively nearby region. Hence it is helpful to identify nearby cosmic ray (CR) sources by observation as well as to understand the processes of acceleration and transport of CREs. Moreover, the anomalies of CREs are also viewed as a smoking gun for dark matter annihilation or decay. In particular, the increase of CR positron fraction above 10 GeV [1–9] has sparked strong interest from particle physicists, leading to many endeavors to account for its origin in dark matter (see Ref. [10] and references therein).

Thanks to progress in detector technology, the spectrum of CREs is now measured accurately to TeV energies and more structures have been uncovered. Multiple studies [11–14] address the apparent primary electron excess above 100 GeV, which resembles the hardening of CR nuclei above $\sim$200 GV [15–21]. This discovery has been established by the up-to-date observations of the Fermi-LAT [22] and DAMPE [23] satellites, both of which show that the total electron spectrum can be fitted well by a broken power-law, with a breaking energy $E_{\rm br}\sim 50$ GeV. The possible origins of electron hardening usually boil down to local source effects [13, 24] or non-linear acceleration processes [25].

Meanwhile, a knee-like structure in the total electron spectrum at $\sim$ TeV energies has been observed. This sharp steepening of CRE flux was initially reported by the H.E.S.S. collaboration [26, 27] and soon afterwards, other ground-based experiments, e.g. MAGIC [28] and VERITAS [29], confirmed the feature. At around 1 TeV, the spectral index changes from ~ -3.0 to ~ -4.1, which is much like the CR knee appearing at $\sim$4 PeV [30, 31]. However, subject to the sizeable systematic uncertainties of indirect measurements, the accurate position of the breaking energy is still in dispute. The DAMPE space experiment has measured the TeV break of CREs accurately, with excellent high energy resolution and low

Received 22 March 2018, Published online 5 June 2018

* Supported by National Natural Sciences Foundation of China (11663006, 11747316, 11135010, 11405182) and the Research Project of Chinese Ministry of Education (213036A)

1) E-mail: liuwei@ihep.ac.cn

2) E-mail: shiying@whu.edu.cn

background [23]. By their precise detection, the spectral break occurs at $\sim$0.9 TeV, with the index varying from ~ -3.1 to ~ -3.9. Several works suggest the knee-like structure in the CRE spectrum may be attributed to the acceleration limit or the confinement at source [32–35], the energy loss during propagation [36, 37], or even the natural outgrowth of nearby sources [24, 38–42]. The knee-like structure may also arise from a threshold interaction of CRs with unknown particle X widespread in the Galaxy [43].

Galactic supernova remnants (SNRs) have been long considered as acceleration sites of CRs below PeV energies, and recent multiwavelength observations from radio to TeV γ-rays have provided abundant evidence [44–47]. Measurements of their radio emissions show that the inferred spectral indices of accelerated charged particles are not a uniform value, but have a remarkable dispersion [48]. Thus, given the available observations, it is plausible that the actual injection spectra of different CR sources are also different. In this work, we propose that the observed total electron spectrum results from a superposition of a host of CR sources with a dispersion of injection spectrum indices ν and cutoff energies E_c. In fact, a similar motivation has been developed to resolve the so-called "GeV excess" puzzle of Galactic diffuse gamma rays observed by EGRET [49, 50]. It has also been used successfully to explain the spectral hardening of CR nuclei above 200 GeV [51]. To interpret the spectrum, the injection power index ν is assumed to obey Gaussian distribution, while the cut-off energy E_c follows a power-law. Under the above assumptions, the total electron spectrum within a wide energy range can be reproduced well.

The rest of the paper is organized as follows. In Section **2**, we give an introduction to the model. The results are presented in Section **3**. Finally, Section **4** gives some discussion and our conclusions.

2 Model description

The spectral hardening induced by the distributed power indices can be understood as follows [51]. The injection spectrum of each source is simply hypothesized as a single power law of rigidity, i.e. $(\mathcal{R}/\mathcal{R}_n)^{-\nu}$, with the power index ν having an even probability distribution between ν_1 and ν_2, i.e.

$$p(\nu)=\frac{1}{\nu_2-\nu_1}. \tag{1}$$

Then the total injection spectrum of CREs is:

$$q(\mathcal{R})=\int_{\nu_1}^{\nu_2}\left(\frac{\mathcal{R}}{\mathcal{R}_n}\right)^{-\nu}p(\nu)\mathrm{d}\nu\propto\left[\left(\frac{\mathcal{R}}{\mathcal{R}_n}\right)^{-\nu_1}-\left(\frac{\mathcal{R}}{\mathcal{R}_n}\right)^{-\nu_2}\right]$$

$$\propto\left(\frac{\mathcal{R}}{\mathcal{R}_n}\right)^{-\nu_2}\left[\left(\frac{\mathcal{R}}{\mathcal{R}_n}\right)^{\nu_2-\nu_1}-1\right]. \tag{2}$$

The break of the spectrum happens at rigidity $\mathcal{R}_n$. When $\mathcal{R}\ll\mathcal{R}_n$, $\left(\frac{\mathcal{R}}{\mathcal{R}_n}\right)^{\nu_2-\nu_1}\ll 1$ and $q(\mathcal{R})$ falls off as $\mathcal{R}^{-\nu_2}$, whereas when $\mathcal{R}\gg\mathcal{R}_n$, $\left(\frac{\mathcal{R}}{\mathcal{R}_n}\right)^{\nu_2-\nu_1}\gg 1$ and $q(\mathcal{R})$ approaches $\mathcal{R}^{-\nu_1}$. Therefore it can be seen that with increasing energy, the spectrum gradually hardens.

To fit the whole spectrum, the injection spectrum of each source is parameterized as a broken power-law of rigidity, that is

$$q(\mathcal{R})=q_0\times\begin{cases}\left(\frac{\mathcal{R}}{\mathcal{R}_{br}}\right)^{-\nu_a}\left(\frac{\mathcal{R}_{br}}{\mathcal{R}_n}\right)^{-\nu_b} & \mathcal{R}\leqslant\mathcal{R}_{br}\\ \left(\frac{\mathcal{R}}{\mathcal{R}_n}\right)^{-\nu_b}\exp\left[-\left(\frac{\mathcal{R}}{\mathcal{R}_c}\right)^{\beta}\right] & \mathcal{R}>\mathcal{R}_{br}\end{cases}. \tag{3}$$

The low-energy electron injection spectrum may be modified by the ion-neutral collisions around shocks [52]. Therefore we add an extra spectral break at $\sim$ GeV, with $\mathcal{R}_{br}$ to be determined by the observational data. Below $\mathcal{R}_{br}$, the spectrum falls off as $\mathcal{R}^{-\nu_\alpha}$. To give a better description of the dispersion of high-energy power index ν_b, it is hypothesized as a Gaussian distribution around a mean value $\bar{\nu}$, namely

$$p(\nu)=\frac{1}{\sqrt{2\pi}\sigma_\nu}\exp\left[-\frac{(\nu-\bar{\nu})^2}{2\sigma_\nu^2}\right], \tag{4}$$

where both $\bar{\nu}$ and its standard deviation σ_ν are evaluated by fitting the CRE spectrum.

The broken power law near the CR knee is usually taken as a superposition of the each elemental spectrum with an exponential cutoff. According to the origins of the exponential cutoff, in other words, astronomical or physical, the cutoff energy E_c of each element could be either $Z-$ or $A-$dependent. Like the CR knee, the TeV break of total electron spectrum could be regarded as a superposition of many sources with a dispersion of cutoff rigidity $\mathcal{R}_c$. Since the observed break of the CRE spectrum is quite sharp, a super-exponential cutoff of each source is assumed, as shown in Eq. (3), with parameter β to be fitted. The cutoff rigidity $\mathcal{R}_c$ is assumed as a power-law distribution, i.e.

$$p(\mathcal{R}_c)\propto\mathcal{R}_c^{-\alpha},\ \ \mathcal{R}_c\in[\mathcal{R}_{c1},\mathcal{R}_{c2}], \tag{5}$$

in which the power index α and the minimum cutoff rigidity $\mathcal{R}_{c1}$ are undetermined parameters.

Taking into account the dispersions of both power index ν and cutoff rigidity $\mathcal{R}_c$, the total injection spectrum thus becomes

$$q(\mathcal{R})=\frac{1}{\int_{\nu_1}^{\nu_2}\exp\left[-\frac{(\nu-\bar{\nu})^2}{2\sigma_\nu^2}\right]\mathrm{d}\nu\int_{\mathcal{R}_{c1}}^{\mathcal{R}_{c2}}\mathcal{R}_c^{-\alpha}\mathrm{d}\mathcal{R}_c}$$
$$\times\int_{\nu_1}^{\nu_2}q_0\left(\frac{\mathcal{R}}{\mathcal{R}_n}\right)^{-\nu}\exp\left[-\frac{(\nu-\bar{\nu})^2}{2\sigma_\nu^2}\right]\mathrm{d}\nu$$
$$\times\int_{\mathcal{R}_{c1}}^{\mathcal{R}_{c2}}\exp\left[-\left(\frac{\mathcal{R}}{\mathcal{R}_c}\right)^\beta\right]\mathcal{R}_c^{-\alpha}\mathrm{d}\mathcal{R}_c\ , \qquad (6)$$

where ν_1 and ν_2 are set to $\bar{\nu}$–$2\sigma_\nu$ and $\bar{\nu}$+$2\sigma_\nu$ respectively, whereas $\mathcal{R}_{c2}$ is fixed to be 100 TV.

To obtain the spectrum of CREs after transport, the numerical package GALPROP* is introduced to solve the transport equation. For a comprehensive introduction to transport of CRs in the Galaxy, one can refer to Refs. [53, 54]. In this work, a pure diffusion model is adopted. Below tens of GeV, the CRE flux is severely impacted by the solar modulation and the well-known force field approximation is applied [55].

3 Results

Figures 1 and 2 illustrate the calculated injection spectrum and the fit to the total electron spectrum respectively. In Fig. 2, the red data points are the total electron spectrum measured by the DAMPE satellite [23], whose energy range is from 25 GeV to 4.6 TeV. Below 25 GeV, the observational data of AMS-02 are used [56] (blue points). Both the injection spectrum and transport parameters are summarized in Table 1. The black solid line is the fit to the electron spectrum. To fit the low energy spectrum, the break energy $\mathcal{R}_{br}$ is set to 8.5 GV, and ν_a is 2.1. The corresponding modulation potential is 480 MeV, which is compatible with the inference from PAMELA observations [16].

The fitted $\mathcal{R}_n$ is 120 GV, which is slightly lower than the excess position of CR nuclei, at $\sim$200 GeV. From Fig. 1, it can be seen that via the integration of Gaussian probability distribution of ν_b, the position of excess moves down to tens of GeV. Furthermore, owing to the energy loss of energetic electrons during the transport, it shifts to about 50 GeV, which is in accordance with the measurements by Fermi-LAT and DAMPE. The same goes for the cutoff rigidity. The fitted minimum cutoff rigidity is 1.2 TV, but the actual cutoff position in the total electron spectrum is less than 1 TeV, which also results from the diffusion effect of CREs.

Moreover, the transport process of CREs effectively smooths out the original injection spectrum. In the initial injection spectrum, the lower energy break at $\sim$8.5 GeV is very sharp, but after the transport, the break becomes smoother. So does the hardening, as well as the high energy cutoff. The average of ν_b is 2.4 and its standard deviation is 0.53. The obtained excess in the injection spectrum grows rapidly with energy, so that it forms a prominent bump above hundreds of GeV. After the transport, the bump disappears and the spectrum flattens.

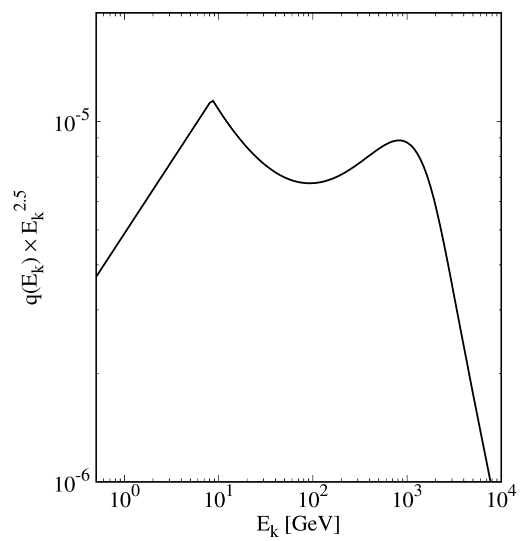

Fig. 1. The total electron injection spectrum computed by Eq. (6) with the corresponding parameters listed in Table 1. The injection spectrum is multiplied by $E_k^{2.5}$.

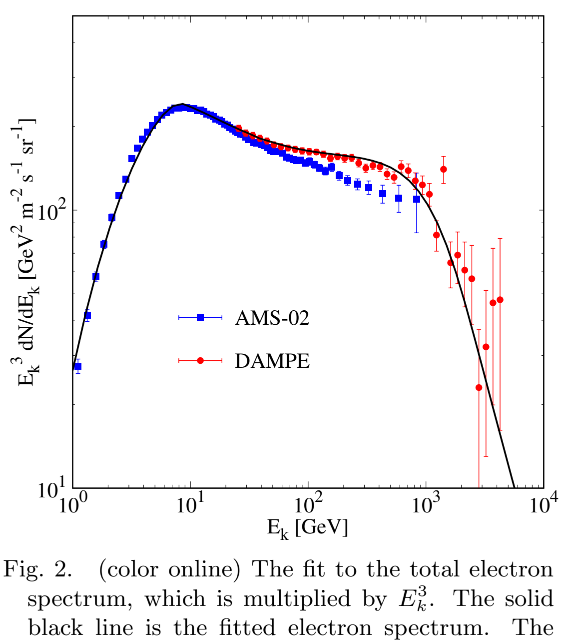

Fig. 2. (color online) The fit to the total electron spectrum, which is multiplied by E_k^3. The solid black line is the fitted electron spectrum. The blue and red data points are taken from AMS-02 [56] and DAMPE [23] respectively. The corresponding parameters are shown in Table 1.

*http://galprop.stanford.edu/

Table 1. Parameters of the transport and injection spectrum. The diffusion coefficient is parameterized as $D_{xx}(\mathcal{R})=D_0(\mathcal{R}/\mathcal{R}_0)^{\delta}$ and L is the half thickness of the diffusive halo. $\bar{\nu}$ and σ_{ν} are the mean value and standard deviation of the distribution of $\nu_{\rm b}$ respectively. Φ is the modulation potential. The normalization flux is set to 1.21×10^{-9} $\rm cm^{-2}\ sr^{-1}\ s^{-1}\ MeV^{-1}$ at 25 GeV.

$D_0/(\rm cm^2/s)$	δ	$\mathcal{R}_0$	L/kpc	$\mathcal{R}_{\rm br}$/GV	$\nu_{\rm a}$	$\mathcal{R}_{\rm n}$/GV
6.58×10^{28}	0.333	4	5	8.5	2.1	120
$\bar{\nu}$	σ_{ν}	$\mathcal{R}_{\rm c1}$/GV	α	β	Φ/MV	
2.44	0.52	1.2×10^3	3	2	480	

Meanwhile, the cutoff of the total electron spectrum is very sharp, compared with the CR knee. Thus, in order to fit the total electron spectrum well, a super-exponential cutoff is required. This is different from the CR knee, in which an exponential cutoff is enough. The super-exponential cutoff is permissible, and several mechanisms have bee proposed to cause variations in the shape of the high-energy cutoff [57–60]. Here we set β equal to 2.

4 Discussion and conclusions

We have demonstrated that both the excess above 50 GeV and the break at TeV energies in the total electron spectrum originate from the superposition of many sources with a dispersion of power index and cutoff energy. To reproduce the observational data, the power index is assumed to have a Gaussian distribution around a mean value, while the cutoff rigidity is assumed to follow a power-law distribution. In addition, due to the sharp break of electron spectrum at TeV energies, a super-exponential cutoff is postulated. In light of the above hypotheses, both the spectral hardening and TeV break can be described well.

Above $\sim$1 TeV, subject to severe energy losses, the lifetime of energetic electrons is less then 3×10^5 years [61] and most of them come from the region $\sim$ 1 kpc away from the solar system. Thus one may consider the assumption of continuous source distribution no longer seems to hold true. Hence both spectral hardening and the TeV break may be dominated by one or two nearby young SNRs or pulsars. However recent work by the HAWC collaboration [62] indicates that due to relatively slow diffusion around the source region, one or two nearby pulsars, e.g. Geminga or PSR B0656+14, could not be adequate to explain the observed positron excess. One solution is that there may be more unknown sources within $\sim$1 kpc around the solar system, which contribute high energy electrons and positrons. Thus the assumption of continuous source distribution may be still valid above 1 TeV.

The authors thank Prof. Qiang Yuan and Dr. Yiqing Guo for helpful discussions and suggestions.

References

1 M. A. DuVernois, S. W. Barwick, J. J. Beatty et al, ApJ, **559**: 296–303 (2001)
2 J. J. Beatty, A. Bhattacharyya, C. Bower et al, Physical Review Letters, **93**(24): 241102 (2004)
3 M. Aguilar, J. Alcaraz et al (AMS-01 Collaboration), Physics Letters B, **646**: 145–154 (2007)
4 J. Chang, J. H. Adams, H. S. Ahn et al, Nature, **456**: 362–365 (2008)
5 S. Torii, T. Yamagami, T. Tamura et al, High-energy electron observations by PPB-BETS flight in Antarctica. ArXiv e-prints, September 2008
6 O. Adriani, G. C. Barbarino, G. A. Bazilevskaya et al, Nature, **458**: 607–609 (2009)
7 A. A. Abdo, M. Ackermann, M. Ajello et al, Physical Review Letters, **102**(18): 181101 (2009)
8 L. Accardo, M. Aguilar, D. Aisa et al, Physical Review Letters, **113**(12): 121101 (2014)
9 M. Aguilar, D. Aisa, A. Alvino et al, Physical Review Letters, **113**(12): 121102 (2014)
10 X.-J. Bi, P.-F. Yin, and Q. Yuan, Frontiers of Physics, **8**: 794–827 (2013)
11 I. Cholis and D. Hooper, Phys. Rev. D, **88**(2): 023013 (2013)
12 Q. Yuan and X.-J. Bi, Physics Letters B, **727**: 1–7 (2013)
13 L. Feng, R.-Z. Yang, H.-N. He et al, Physics Letters B, **728**: 250–255 (2014)
14 X. Li, Z.-Q. Shen, B.-Q. Lu et al, Physics Letters B, **749**: 267–271 (2015)
15 A. D. Panov, J. H. Adams, H. S. Ahn et al, Bulletin of the Russian Academy of Sciences, Physics, **73**: 564–567 (2009)
16 O. Adriani, G. C. Barbarino, G. A. Bazilevskaya et al, Science, **332**: 69 (2011)
17 H. S. Ahn, P. Allison, M. G. Bagliesi et al, ApJl, **714**: L89–L93 (2010)
18 Y. S. Yoon, H. S. Ahn, P. S. Allison et al, ApJ, **728**: 122 (2011)
19 M. Aguilar, D. Aisa, B. Alpat et al, Physical Review Letters, **114**(17): 171103 (2015)
20 M. Aguilar, D. Aisa, B. Alpat et al, Physical Review Letters, **115**(21): 211101 (2015)
21 M. Aguilar, L. Ali Cavasonza, G. Ambrosi et al, Phys. Rev. Lett., **120**: 021101 (2018)
22 S. Abdollahi, M. Ackermann, M. Ajello et al, Phys. Rev. D, **95**(8): 082007 (2017)
23 DAMPE Collaboration, G. Ambrosi, Q. An et al, Nature, **552**: 63–66 (2017)
24 W. Liu, X.-J. Bi, S.-J. Lin, B.-B. Wang, and P.-F. Yin, Phys. Rev. D, **96**(2): 023006 (2017)
25 V. Ptuskin, V. Zirakashvili, and E.-S. Seo, ApJ, **763**: 47 (2013)
26 F. Aharonian, A. G. Akhperjanian, U. Barres de Almeida et al, Physical Review Letters, **101**(26): 261104 (2008)
27 F. Aharonian, A. G. Akhperjanian, G. Anton et al, A&A, **508**: 561–564 (2009)

28 D. Borla Tridon, International Cosmic Ray Conference, **6**: 47 (2011)
29 D. Staszak (VERITAS Collaboration), In 34th International Cosmic Ray Conference (ICRC2015), volume 34 of International Cosmic Ray Conference, page 411, July 2015
30 M. Amenomori, X. J. Bi, D. Chen et al, ApJ, **678**: 1165–1179 (2008)
31 M. G. Aartsen, R. Abbasi, Y. Abdou et al, Phys. Rev. D, **88**(4): 042004 (2013)
32 G. Vannoni, S. Gabici, and F. A. Aharonian, A&A, **497**: 17–26 (2009)
33 S. Thoudam and J. R. Hörandel, MNRAS, **414**: 1432–1438 (2011)
34 Y. Ohira, R. Yamazaki, N. Kawanaka, and K. Ioka, MNRAS, **427**: 91–102 (2012)
35 K. Fang, X.-J. Bi, and P.-F. Yin, ApJ, **854**: 57 (2018)
36 R. Schlickeiser and J. Ruppel, New Journal of Physics, **12**(3): 033044 (2010)
37 Ł. Stawarz, V. Petrosian, and R. D. Blandford, ApJ, **710**: 236–247 (2010)
38 N. Kawanaka, K. Ioka, and M. M. Nojiri. Is Cosmic Ray Electron Excess from Pulsars Spiky or Smooth?: Continuous and Multiple Electron/Positron Injections. ApJ, 710:958–963, February 2010.
39 K. Fang, B.-B. Wang, X.-J. Bi, S.-J. Lin, and P.-F. Yin, ApJ, **836**: 172 (2017)
40 B.-B. Wang, X.-J. Bi, S.-J. Lin, and P.-f. Yin, Explanations of the DAMPE high energy electron/positron spectrum in the dark matter annihilation and pulsar scenarios, ArXiv e-prints, July 2017
41 Q. Yuan, L. Feng, P.-F. Yin et al, Interpretations of the DAMPE electron data, ArXiv e-prints, November 2017
42 K. Fang, X.-J. Bi, P.-F. Yin, and Q. Yuan, Two-zone diffusion of electrons and positrons from Geminga explains the positron anomaly, ArXiv e-prints, March 2018
43 C. Jin, W. Liu, H.-B. Hu, and Y.-Q. Guo, On the PeV knee of cosmic rays spectrum and TeV cutoff of electron spectrum, ArXiv e-prints, November 2016
44 S. P. Reynolds, ARA&A, **46**: 89–126 (2008)
45 G. Dubner and E. Giacani, A&A Rev., **23**: 3 (2015)
46 P. Slane, A. Bykov, D. C. Ellison, G. Dubner, and D. Castro, Space Sci. Rev., **188**: 187–210 (2015)
47 A. M. Bykov, D. C. Ellison, A. Marcowith, and S. M. Osipov, Space Sci. Rev., **214**: 41 (2018)
48 D. A. Green, Bulletin of the Astronomical Society of India, **42**: 47–58 (2014)
49 M. Pohl and J. A. Esposito, ApJ, **507**: 327–338 (1998)
50 I. Büsching, M. Pohl, and R. Schlickeiser, A&A, **377**: 1056–1062 (2001)
51 Q. Yuan, B. Zhang, and X.-J. Bi, Phys. Rev. D, **84**(4): 043002 (2011)
52 M. A. Malkov, P. H. Diamond, and R. Z. Sagdeev, Nature Communications, **2**: 194 (2011)
53 D. Maurin, R. Taillet, F. Donato et al, Galactic Cosmic Ray Nuclei as a Tool for Astroparticle Physics, ArXiv Astrophysics e-prints, December 2002
54 A. W. Strong, I. V. Moskalenko, and V. S. Ptuskin, Annual Review of Nuclear and Particle Science, **57**: 285–327 (2007)
55 L. J. Gleeson and W. I. Axford, ApJ, **154**: 1011 (1968)
56 M. Aguilar, D. Aisa, B. Alpat et al, Physical Review Letters, **113**(22): 221102 (2014)
57 E. G. Berezhko and G. F. Krymskiǐ, Soviet Physics Uspekhi, **31**: 27–51 (1988)
58 P. A. Becker, T. Le, and C. D. Dermer, ApJ, **647**: 539–551 (2006)
59 V. N. Zirakashvili and F. Aharonian, A&A, **465**: 695–702 (2007)
60 P. Blasi, MNRAS, **402**: 2807–2816 (2010)
61 T. Kobayashi, Y. Komori, K. Yoshida, and J. Nishimura, ApJ, **601**: 340–351 (2004)
62 A. U. Abeysekara, A. Albert, R. Alfaro et al, Science, **358**: 911–914 (2017)